

Analysis of One-Way Fluid-Structure Interactions for a Straight Pipe under Different Thermal and Pressure Conditions

Gökhan CANBOLAT*¹ ORCID 0000-0001-6491-095X

¹Alanya Alaaddin Keykubat University, Department of Mechanical Engineering,
Antalya, Türkiye

Geliş tarihi: 21.09.2023 Kabul tarihi: 25.12.2023

Atıf şekli/ How to cite: CANBOLAT, G., (2023). Analysis of One-Way Fluid-Structure Interactions for a Straight Pipe under Different Thermal and Pressure Conditions. Cukurova University, Journal of the Faculty of Engineering, 38(4), 1049-1060.

Abstract

Numerical studies on stress, deformation, and damages due to fluid flow have been highly carried out using Fluid-Structure Interaction (FSI) in recent years. FSI is highly efficient in investigating a solid domain deformed by the fluid flow. In this study, a one-way fluid-structure interaction study is performed by a straight pipe under different pressure and thermal conditions. Here, the thermophysical properties of the fluid and mechanical properties of the solid domain can be subjected to change during fluid flow. An aluminum straight pipe with a 1 mm wall thickness is operated under 1 Bar, 5 Bar, and 10 Bar with three different surface temperatures -10°C, 20°C, and 50°C. This study aims to investigate the structural variation of aluminum by the temperature and pressure change of operating fluid in the pipe. Variation of thermophysical properties of fluid by heated pipe surface is integrated into the numerical analysis by generated functions. Numerical analysis showed that the variation of temperature in operating fluid highly affects the fluid characteristic and the structural response of the solid domain by different temperatures. An increase in the operating pressure caused maximum deformation to approximately %100 from 1 Bar to 5 Bar, and approximately %120 from 1 Bar to 10 Bar for the adiabatic process as expected but in the heating conditions stress is nearly three times higher than cooling conditions. As a result, one-way FSI solutions are highly effective in investigating the deformed solid domain as a result of flow, thermal, and operating conditions.

Keywords: Structural response, Deformation, Heating, Adiabatic, Fluid-structure interaction

Farklı Isı ve Basınç Koşulları Altında Düz Bir Boru İçin Tek Yönlü Akışkan-Yapı Etkileşimleri Analizi

Öz

Son yıllarda, tek yönlü Akışkan Yapı Etkileşimleri (AYE) ile akış karakteristiklerinin yol açtığı gerilim, deformasyon ve hasarlar üzerine birçok nümerik çalışmalar yapılmıştır. AYE, akış koşulları ile deforme olan bir katı cisim araştırmak için oldukça verimlidir. Bu çalışmada, farklı basınç ve termal koşullar altında düz bir boru içindeki akışta tek yönlü akışkan yapı etkileşimi analizleri gerçekleştirilmiştir. Burada

*Sorumlu yazar (Corresponding Author): Gökhan CANBOLAT, gokhan.canbolat@alanya.edu.tr

akışkanın termofiziksel özellikleri ve katı bölgenin mekanik özellikleri akış sırasında değişime uğrayabilmektedir. 1 mm et kalınlığına sahip alüminyum düz bir boru 1 Bar, 5 Bar ve 10 Bar'lık basınçlar altında ve ayrıca yüzey sıcaklığı -10°C, 20°C ve 50°C olmak üzere farklı operasyon koşullarında analiz edilmiştir. Bu çalışmada boru içerisindeki akışkanın sıcaklık ve basınç değişimi ile alüminyumun yapısal değişiminin araştırılması amaçlanmıştır. Isıtılan boru yüzeyi ile akışkanın termofiziksel özelliklerinin değişimi, oluşturulan fonksiyonlarla sayısal analize entegre edilmiştir. Sayısal analiz, akışkandaki sıcaklık değişiminin, akışkan karakteristiğini ve katı bölgenin yapısal tepkisini farklı sıcaklıklar da oldukça etkilediğini göstermiştir. Çalışma basıncındaki artış ile deformasyondaki maksimum artış beklenildiği gibi adyabatik duruma göre 1 Bar'dan 5 Bar'a yaklaşık %100, 1 Bar'dan 10 Bar'a ise yaklaşık %120'ye ulaşmıştır. Ancak ısıtma koşullarında oluşan gerilimin, soğutma koşullarına göre yaklaşık üç kat daha fazla saptanmıştır. Sonuç olarak tek yönlü FSI çözümlerinin akış, ısı ve çalışma koşulları altında deforme olan katı bölgenin incelenmesinde oldukça etkili olduğunu gösterilmiştir.

Anahtar Kelimeler: Yapısal tepki, Deformasyon, Isıtma, Adyabatik, Akışkan yapı etkileşimi

1. INTRODUCTION

Conveying fluids in pipes are commonly used in many engineering fields such as mechanical, nuclear, marine, civil, petroleum, and electric. In many applications, some failures may occur due to variations in fluid flow and thermal operating conditions. Here, variation of flow characteristic effects directly the solid domain under different operating conditions. Therefore, the interactions between fluid flow and solid domain with the pressure that occurred by the flow need to be taken into account during flow [1].

Fluid-structure interaction is a method that investigates deformation, stress, and failures in the solid domain due to the fluid flow. These interactions can occur in many natural phenomena and the system designed by the engineers. Fluid-structure interaction can be also defined as the interaction between rigid and deformable structures with internal or external flows and it is also a branch related to the loads that occur by the flow with the structural response [2]. In the piping systems, various dynamics forces occur. These forces may move the piping systems and deform so fluid and solid domains can not be solved separately in the engineering approach. FSI is an important method during engineering design with its multidisciplinary advantages [3-5].

One way of fluid-structure interaction is the workflow that results from the fluid model transfers to the solid domain as an external or internal load.

For one way fluid-structure interaction, fluid flow is calculated till the convergence criteria. The forces calculated from the fluid flow at the boundary are transferred to the solid domain. After that structure domain is solved till the convergence criteria of solid mechanics [6-7].

Various FSI studies on pipe flows are performed in the literature from various perspectives. In the study, a fluid-structure interaction study is performed to investigate a water hammer with a thick-wallet pipe. The model of the study is based on conventional water-hammer with beam theories. The governing equations of straight pipes are derived according to the cross-sectional area by two-dimensional basic equations. They revealed that the FSI method is highly effective in pipe flow [8]. In a study, the FSI method is used in straight pipeline systems during the hydraulic transient. The interaction mechanism is modeled by the Poisson, friction, and junction coupling. The resistance due to the movement by inertia and dry friction is coupled with junction coupling. They concluded that the FSI solver is capable of resistance to the movement of straight pipelines [9]. In a study, it is specified that pipes are used to transport high velocity or pressurized fluid generally under different operating conditions. Therefore vibration problems highly occur in the piping system. It is aimed at the study that determines the behavior of fluid flow to valve closure excitation by the FSI method. It is concluded that structural velocity reduces when the FSI effects are taken into account in piping systems with fluid transients by valve

closure excitation [10]. In a study, the FSI method is used to assess flow erosion and deformation of pipes used in oil transportation. This study aims to investigate deformation, stress, and flow conditions. It is concluded that the flow field and deformation of the pipe are highly important for the structural domain [11]. In a study, the slug characteristics of crude oil grades were investigated numerically to assess the effect of change in the stresses. The study was performed by fluid-structure interactions with the horizontal carbon steel pipes. It is found that the increase in the density of the crude oil leads to the formation of slugs close to the inlet side of the tube with high velocities [12]. In a study, deformation and flow erosion in a pipe flow re investigated numerically in a gas-solid flow. Three-dimensional RANS equations are used to carry out the study of the motion of the continuous fluid phase. The FSI method is used for the analysis to calculate deformation. They concluded that erosion rate and deformation are connected to structural changes and inlet conditions [13]. In a study, a pipe flow is studied by using FSI to observe local damages. Poisson, friction, and joints were investigated by the different supports. They concluded that different supports caused the various structural responses [14].

In this study, a pipe with 50 mm diameter, 1000 mm length, and 1 mm thickness is analyzed by FSI. It is specified in various studies in the literature that the FSI method is highly effective in guiding deformation and stress in fluid-solid flows. A straight pipe that is aluminum is investigated under three different inlet pressures and three different surface temperatures. Here, the surface temperature of the wall is 263 K, 293 K, and 323 K while the fluid is at 293 K. The adiabatic case is also analyzed and the differences are shown in the study. The change in thermophysical properties of the fluid by the temperature in terms of density and viscosity is taken into account during the flow. The mesh sensitivity test is performed to obtain a sufficient mesh element number according to Wall Shear Stress (WSS) and y^+ . Results show that variations in the thermophysical properties of the fluid are quite dominant in deformation and stress that occur by solid domain. Here, deformations are between

the range of 0–0.0005 mm, 0.0005–0.001 mm, and 0.01–0.012 mm for adiabatic cases at 1 Bar, 5 Bar, and 10 Bar respectively.

2. MATERIAL AND METHOD

Geometry, generation of mesh, mesh sensitivity test, boundary conditions, governing equations, and numerical methods are presented in this section.

2.1. Domains, Mesh, and Mesh Sensitivity Test

Figure 1. shows the used geometry in numerical analyses. Here, the length (L) of the pipe is 1000 mm, the diameter (D) of the pipe is 50 mm, and the thickness (t) of the solid domain is 1 mm. As it is known, the length of the pipe needs to be a minimum of 10 times the diameter of the pipe for a turbulent flow [15]. For this reason, the pipe length is constructed as 20 times the diameter to obtain the fully developed flow in this turbulent flow. Here, the z direction is the flow direction in the coordinate system and the center of the pipe is constructed to the center of the coordinate system.

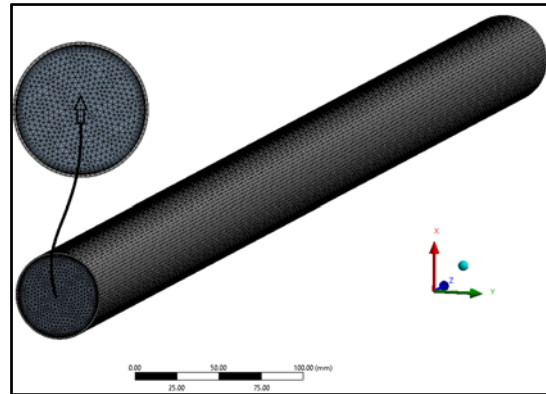


Figure 1. Mesh for the pipe and fluid domain

The generated mesh is shown in Figure 1 by using Ansys Fluent. The fluid domain is meshed by the triangular elements and the hexahedron mesh type is used for the solid domain. An important step is the mesh generation in a numerical analysis. A sufficient mesh element number is needed to be determined by the mesh sensitivity test. y^+ value and WSS are commonly used during the mesh generation [16–18].

Figure 2. shows the mesh sensitivity test performed in this study. As is shown, the mesh sensitivity test is performed according to WSS and y^+ values. When the blue bars indicate the y^+ values, orange bars indicate the WSS values. Here, the y^+ value is the dimensionless number to measure the distance of the first cell to the surface. Changing element size is combined with the seven different mesh element numbers. The first mesh is constructed with an 185025 mesh element number, and it is increased gradually to 3640452 element number. In the first mesh, the y^+ value is nearly 3.3 however it is decreased to 1.1 with the increase in element number. According to Figure 2., the change in WSS and y^+ values decreased after the mesh element number 2080735. So it is determined that the element number 2080735 is sufficient to perform numerical calculations. Here, an increase in element number does not affect the y^+ and WSS values. 9-layer inflation is used close to the pipe wall to predict the boundary layer in detail with a 1.2 growth rate. In this study, structural response and WSS are mainly investigated so a dense mesh is needed in the boundary layer [19].

So it is concluded that this mesh element number is sufficient to perform numerical analyses with a 1 mm element size. Thus it is avoided to perform the numerical calculation with the insufficient mesh

element number and it is also avoided the computational cost with large mesh element numbers.

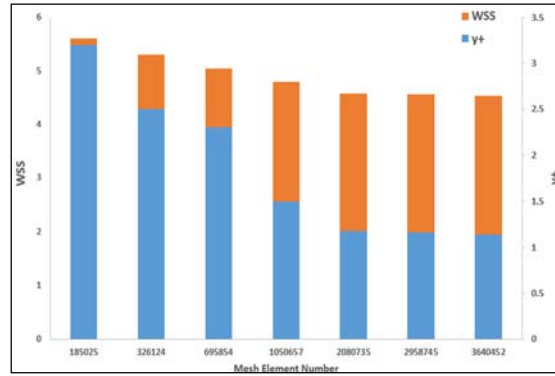


Figure 2. Sensitivity test for the constructed mesh

2.2. Boundary Conditions, Numerical Approach, and Governing Equations

In this study, an incompressible, fully developed, and homogeneous flow is analyzed. No slip boundary condition is implemented at the wall. The interface surface is the inner wall of the pipe for the fluid-structure interactions. So data transfer is provided from this surface as pressure to the solid domain. numbers.

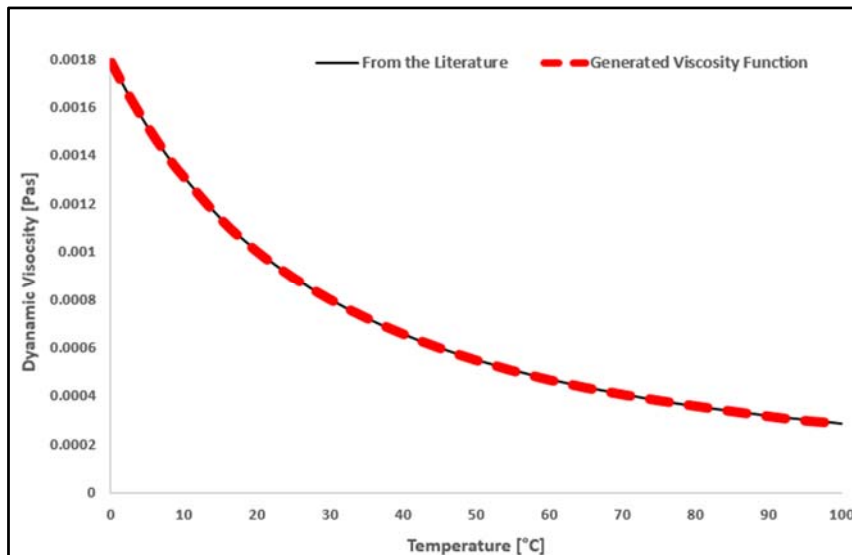


Figure 3. Comparison of generated viscosity function with the data from the literature [15]

Figure 3 shows the generated viscosity function of the water used in this numerical study as fluid. In this study, the viscosity of the water is changed with temperature because of different surface temperatures implemented on the pipe surface. A viscosity function is generated by using data of the

water according to temperature versus viscosity from the literature by using the Matlab Curve Fitting tool. Here, the Fourier Series is used to reflect the viscosity change of water by temperature. The general Fourier Series is shown below.

$$f(x) = a_0 + \sum_{n=1}^{\infty} \left(a_n \cos \frac{n\pi x}{L} + b_n \sin \frac{n\pi x}{L} \right) \quad (1)$$

where,

$$a_0 = \frac{1}{\pi} \int_{-\pi}^{\pi} f(x) dx \quad (2)$$

$$a_n = \frac{1}{\pi} \int_{-\pi}^{\pi} f(x) \cos(n x) dx \quad (3)$$

$$b_n = \frac{1}{\pi} \int_{-\pi}^{\pi} f(x) \sin(n x) dx \quad (4)$$

By using the Fourier Series, a viscosity function is generated from n=1 to n=3. This generated function is integrated into Ansys to take into account variation of viscosity. The generated viscosity function is shown below.

$$\mu(T) = a_0 + a_1 * \cos(T*w) + b_1 * \sin(T*w) + a_2 * \cos(2*T*w) + b_2 * \sin(2*T*w) + a_3 * \cos(3*T*w) + b_3 * \sin(3*T*w) \quad (5)$$

The coefficients of the Fourier Series generated for the viscosity are $a_0=0.004028$, $a_1=-0.0006304$, $b_1=-0.005247$, $a_2=-0.001862$, $b_2=0.0008052$, $a_3=0.0002512$, $b_3=0.0002638$, and $w = 0.02094$ respectively. T is temperature and μ is the dynamics viscosity in the function.

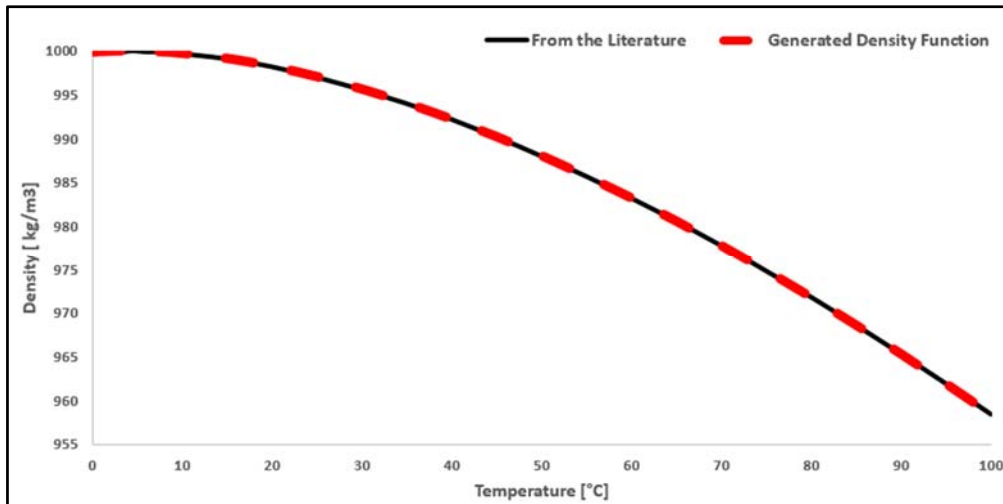


Figure 4. Comparison of generated density function with the data from the literature [15]

By using the Fourier Series, a density function is generated from n=1 to n=3. This generated function is integrated into Ansys to take into account variation of density. The generated density function is shown below.

$$\rho(T) = a_0 + a_1 * \cos(T*w) + b_1 * \sin(T*w) + a_2 * \cos(2*T*w) + b_2 * \sin(2*T*w) + a_3 * \cos(3*T*w) + b_3 * \sin(3*T*w) \quad (6)$$

The coefficients of the Fourier Series generated for the viscosity are $a_0=957.1$, $a_1=41.47$, $b_1=17.54$, $a_2=2.066$, $b_2=-6.523$, $a_3=-0.757$, $b_3=-0.3782$, and $w=0.02009$. T is the temperature and ρ is the density in the function.

The variation of the viscosity and the density of the water by temperature is integrated with the numerical analyses mentioned above. In this way,

the change in fluid characters is considered for the pipe flow. Otherwise, the variation of viscosity and density changes the numerical results then the transferred data from the fluid domain to the solid domain may not reflect the actual values.

Table 1 shows the thermophysical properties of the water used as the fluid in this numerical study. Density and viscosity are specified in Figure 3 and Figure 4 because of changes in the temperature. So it can not accept constant density and viscosity for the fluid in this study. Here, the change in thermal conductivity and the specific heat by temperature are ignored.

Table 1. Thermophysical properties of the fluid

Density	Figure 4	kg/m ³
Viscosity	Figure 3	MPa
Thermal conductivity	0.6	W/m-K
Specific heat	4182	J/kg-K

Table 1. Mechanical properties of the aluminum

Density	2719	kg/m ³
Young's modulus	71000	MPa
Thermal conductivity	237	W/m-K
Specific heat	871	J/kg-K
Poisson ratio	0.33	
Bulk modules	69608	MPa
Tensile ultimate strenght	310	MPa

Table 2 shows the mechanical properties of the Aluminum used in this study as the solid domain. The change in properties of the solid domain is ignored. The variation of fluid properties is taken into account and the effects of this variation are investigated in this study.

$$Re = \frac{\rho U D_h}{\mu} \tag{7}$$

The ratio of the inertial forces to viscous force is defined as the Reynolds (Re) number. Here, U , ρ , μ , and D_h are velocity [m/s], density [kg/m³], dynamic viscosity [Pas], and characteristic length [m]. In this study, high pressures are implemented on a pipe with a small diameter so Re numbers are highly large and this is a turbulent flow due to Reynolds numbers of 647000, 1200000, and 1900000 for the 1 Bar, 5 Bar, and 10 Bar respectively.

One-way FSI is used so ALE approach is needed to couple of fluid mechanics and solid mechanics. The equation of Cauchy's law for motion is derived to balance the forces. The product of the velocity and density is balanced with the divergence of the stress tensor and other body forces.

$$\rho \left[\frac{\partial \mathbf{u}}{\partial t} + \mathbf{u} \cdot \nabla \mathbf{u} \right] = \nabla \cdot \sigma + \mathbf{f} \tag{8}$$

where ρ is the solid density, \mathbf{u} is the velocity vector, σ is the Cauchy stress tensor, and \mathbf{f} is the external body force. The displacement of the fluid-solid interface and fluid domain is derived from the ALE configuration [20].

$$\rho_f \left[\frac{\partial \mathbf{u}_f}{\partial t} + \mathbf{u}_f \cdot \nabla \mathbf{u}_f \right] = -\nabla p + \mu \nabla^2 \mathbf{u}_f \tag{9}$$

$$\nabla \cdot \mathbf{u}_f = 0 \tag{10}$$

where ρ_f is the fluid density, \mathbf{u}_f is the velocity vector, μ is the dynamic viscosity, and p is the pressure in the fluid domain.

$$\rho_s \frac{\partial^2 \mathbf{d}_s}{\partial t^2} = \nabla \cdot \sigma_s \tag{11}$$

where,

\mathbf{d}_s is the solid displacement, ρ_s solid density, σ_s is the Cauchy stress in the tube. The forces and velocities must be equal in the fluid-structure interface.

$$\mathbf{u}_f = \mathbf{u}_s \text{ at the interface of fluid-structure} \tag{12}$$

$$\sigma_s \cdot \mathbf{n} = \Gamma \cdot \mathbf{n} \tag{13}$$

where,

σ_s is the Cauchy stress tensor, \mathbf{n} is the unit normal, and Γ is the real stress.

In this study, the SST k- ω model was used to predict the turbulent flow. Transport equations for the SST k- ω model;

$$\frac{\partial(\rho k)}{\partial t} + \frac{\partial(\rho k u_i)}{\partial x_i} = \frac{\partial}{\partial x_j} \left[\Gamma_k \frac{\partial k}{\partial x_j} \right] + G_k - Y_k + S_k \tag{14}$$

$$\frac{\partial(\rho\omega)}{\partial t} + \frac{\partial(\rho\omega u_i)}{\partial x_i} = \frac{\partial}{\partial x_j} \left[\Gamma_\omega \frac{\partial\omega}{\partial x_j} \right] + G_\omega - Y_\omega + D_\omega + S_\omega \quad (15)$$

k and ω are the kinetic energy and specific dissipation rate in the SST $k-\omega$ turbulent model. G_k is defined as the generation of turbulence kinetic energy. G_ω is the generation of ω . Γ_ω and Γ_k are the effective diffusivity of ω and k , respectively. Y_ω and Y_k and are the dissipation of ω and k . S_k and S_ω are user-defined source terms in Equation [4,21].

All the second-order upwind discretization is used during the numerical simulation to discretize the momentum, turbulent kinetic energy, pressure, and turbulent dissipation rate. The criteria for the convergence is chosen 10^{-5} in the residuals. Steady-state and 3D flow analyses are performed.

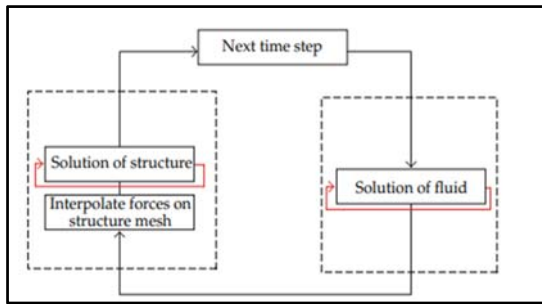


Figure 5. Algorithm of the one-way coupling FSI [6]

Figure 5 shows the algorithm of one-way FSI. In this model, the fluid domain is highly thrilled by structural deformations. In this way, structural calculations and CFD can be solved independently with data transfer. In the one-way coupling algorithm, only fluid pressure is transferred to the structural domain from the fluid domain [22].

3. RESULTS AND DISCUSSION

In this study, the main purpose is to investigate deformation and Von Mises stress according to changing flow parameters. The parameters such as

deformation and Von Mises stress are related to both the thermophysical properties of the fluid and elastic properties of the material in a coupled flow structure analysis. The pressure of 1 Bar, 5 Bar, and 10 Bar is implemented for the inlet of the pipe. Heating and cooling effects on the surface of the solid domain are studied with the same temperature of the fluid for the solid wall. The changing thermophysical parameters for the density and viscosity are used for the fluid to assess the effect of deformation and Von Mises stress. Fluid is at the temperature of 293 K in all cases and the surface of the solid domain is 263 K for cooling and 323 K for heating. Here, results are shown for the along the pipe length for these nine cases.

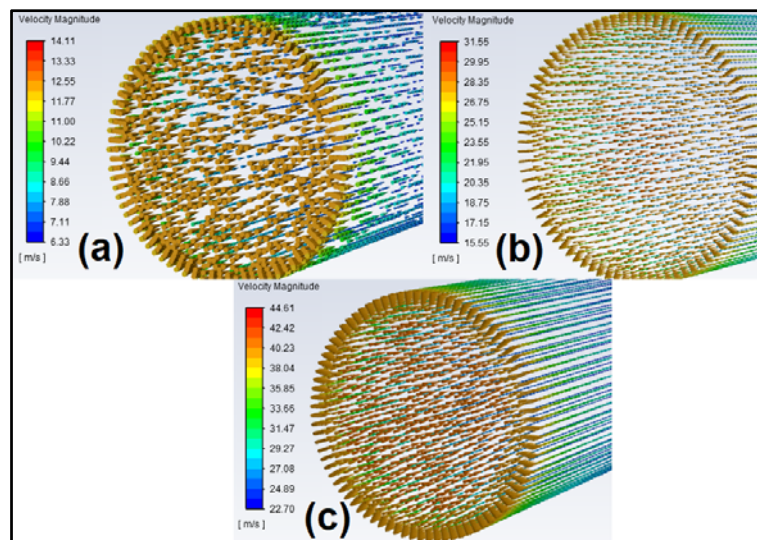


Figure 6. Velocity vectors of the inlet for different pressures a) 1 Bar, b) 5 Bar, and c) 10 Bar

Figure 6 shows the velocity vectors for the adiabatic cases solved in this study. Here fluid is at 293 K. The inlet velocities are around 13 m/s, 26 m/s, and 39 m/s.

The turbulent flow occurs in the pipe in all cases as mentioned by Re numbers. The velocity increases with an increase in pressure implemented for the inlet as expected.

The velocity contours present the flow paths here. Figure 7 presents the variation of the deformation by the constant surface temperature of the solid surface at the pressure of 1 Bar. Here, there are three thermal conditions they are heating at 323K, cooling at 263 K, and in the adiabatic case, there is no heat transfer. In the adiabatic case, the fluid at 293 K, and the surface is 293 K also. So there is no heat transfer here, energy equations are not solved

in this case. Here, the deformation is almost none for the adiabatic case. It is in the range of 0 – 0.0005 mm. However, the deformation is highly large for the heating and cooling cases. It is in the range of 0.012 mm – 0.014 mm in the middle of the pipe.

Figure 8 presents the variation of the Von Mises stress by the constant surface temperature of the solid surface at the pressure of 1 Bar. Here, there are three thermal conditions they are heating at 323K, cooling at 263 K, and in the adiabatic case, there is no heat transfer. In the adiabatic case, the fluid at 293 K, and the surface is 293 K also. So there is no heat transfer here, energy equations are not solved in this case. As it is seen, Von Mises stress is highly low for the adiabatic case. However, the stress is highly large for the heating and cooling cases. It is nearly 8 MPa for the cooling case and it is nearly 16 MPa for the heating case along the pipe. cases.

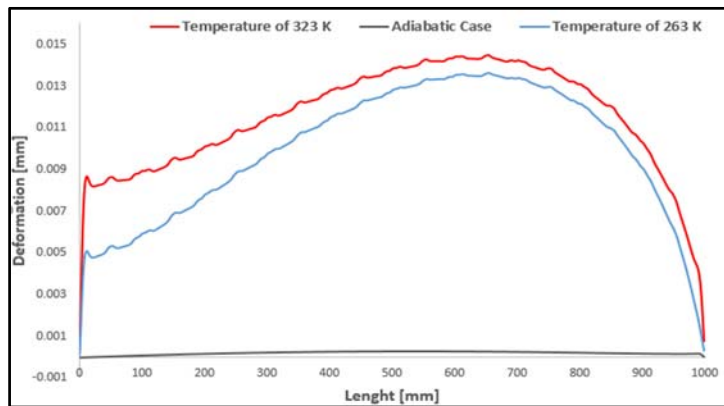


Figure 7. Deformations at the pressure of 1 Bar

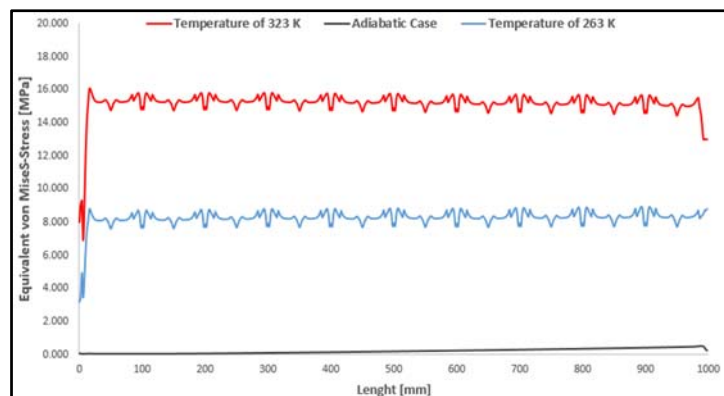


Figure 8. Von Mises stress at the pressure of 1 Bar

Figure 9 presents the variation of the deformation by the constant surface temperature of the solid surface at the pressure of 5 Bar. Here, there are three thermal conditions they are heating at 323K, cooling at 263 K, and in the adiabatic case, there is no heat transfer. In the adiabatic case, the fluid at 293 K, and the surface is 293 K also. So there is no heat transfer here, energy equations are not solved in this case. Here, the deformation increases according to the case of 5 Bar and its range of 0.0005 mm – 0.001 mm in the adiabatic case. When the heating and cooling cases are investigated, the deformation is highly large for the heating and cooling cases. It is in the range of 0.01mm – 0.012 mm in the middle of the pipe.

Figure 10 presents the variation of the Von Mises stress by the constant surface temperature of the solid surface at the pressure of 5 Bar. Here, there are three thermal conditions they are heating at 323K, cooling at 263 K, and in the adiabatic case, there is no heat transfer. In the adiabatic case, the fluid at 293 K, and the surface is 293 K also. So there is no heat transfer here, energy equations are not solved in this case. As it is seen, Von Mises stress is highly low for the adiabatic case. However, the stress is highly large for the heating and cooling cases. It is nearly 6 MPa for the cooling case and it is nearly 13 MPa for the heating case along the pipe.

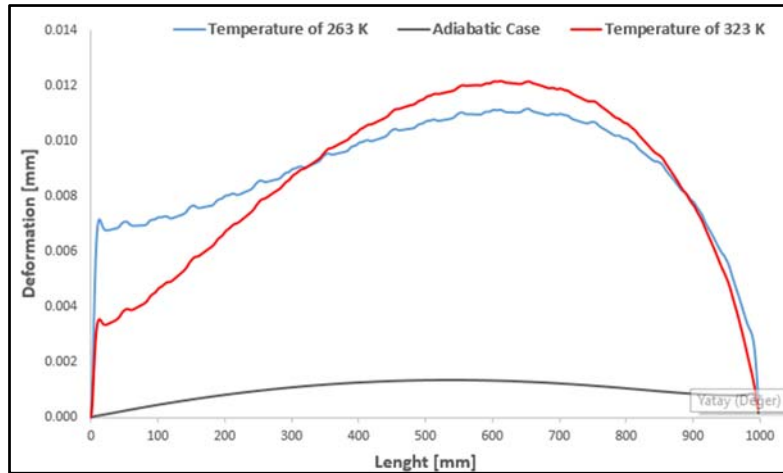


Figure 9. Deformations at the pressure of 5 Bar

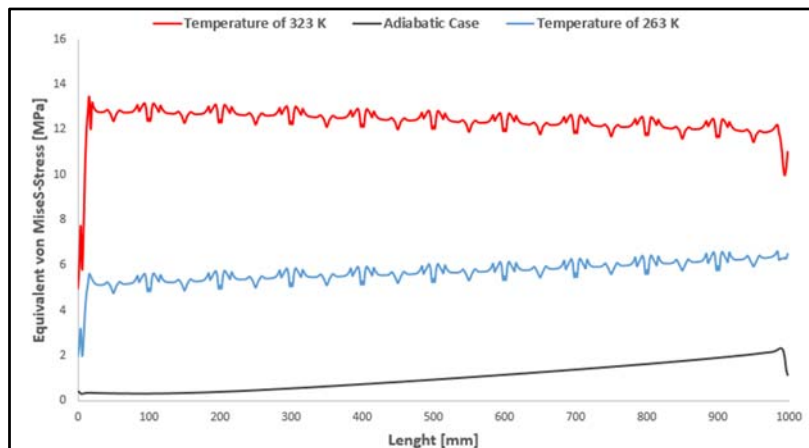


Figure 10. Von Mises stress at the pressure of 5 Bar

Figure 11 presents the variation of the deformation by the constant surface temperature of the solid surface at the pressure of 10 Bar. Here, there are three thermal conditions they are heating at 323K, cooling at 263 K, and in the adiabatic case, there is no heat transfer. In the adiabatic case, the fluid at 293 K, and the surface is 293 K also. So there is no heat transfer here, energy equations are not solved in this case. Here, the deformation increases according to the case of 10 Bar and its range of 0.001 mm – 0.002 mm in the adiabatic case. When the heating and cooling cases are investigated, the deformation is highly large for the heating and cooling cases. It is in the range of 0.01mm – 0.012

mm in the middle of the pipe. Figure 12 presents the variation of the Von Mises stress by the constant surface temperature of the solid surface at the pressure of 10 Bar. Here, there are three thermal conditions they are heating at 323K, cooling at 263 K, and in the adiabatic case, there is no heat transfer. In the adiabatic case, the fluid at 293 K, and the surface is 293 K also. So there is no heat transfer here, energy equations are not solved in this case. As it is seen, Von Mises stress is highly low for the adiabatic case. However, the stress is highly large for the heating and cooling cases. It is nearly 4 MPa for the cooling case and it is nearly 11 MPa for the heating case along the pipe.

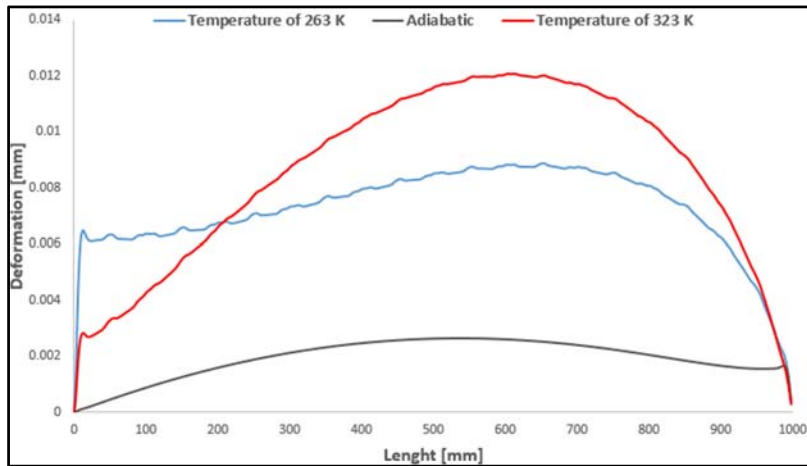


Figure 11. Deformations at the pressure of 10 Bar

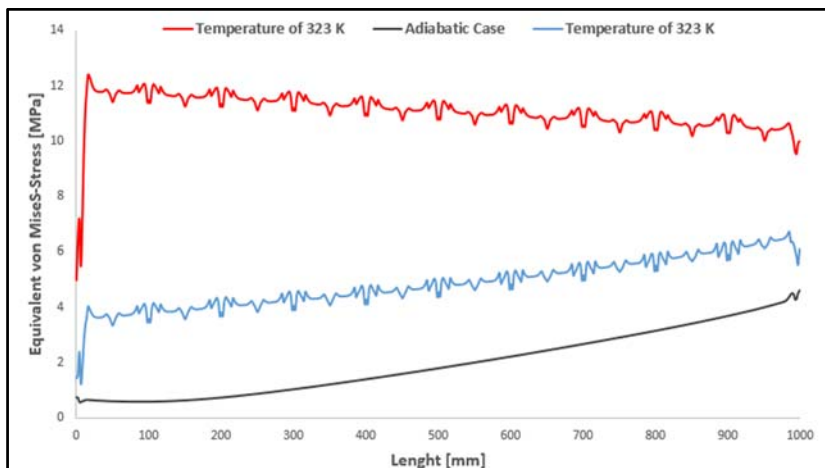


Figure 12. Von Mises stress at the pressure of 10 Bar

FSI analysis showed that deformations and Von Mises stress increase with the increase in pressure as expected for adiabatic cases. However, in all heating or cooling cases, huge differences are observed for the deformation and Von Mises stress due to variations in the thermophysical properties of the fluid. Variation in the thermophysical properties of the fluid affects the flow conditions considerably [23]. The advantages of FSI analysis are obvious according to the pure solid mechanics [24]. Pure solid mechanics calculations may result in lower or larger deformations or stress with unpredictable values [1].

When the figures of deformation and stress are discussed, the sudden rise in these results is observed at the inlet of the pipe. This can be interpreted by developing flow and hydraulic shock when a sudden pressure occurs at the pipe. Here, sudden pressure is a non-stationary flow and sudden change of velocity [25]. Excessive deformation and stress can occur by the abrupt acceleration in a pipe [26].

4. CONCLUSION

In this study, fluid mechanics and solid mechanics are coupled in pipe flow. Straight aluminum pipe is pressurized suddenly with different pressure values as 1 Bar, 5 Bar, and 10 Bar. The deformations and Von Mises stress are investigated under different operating temperatures as heating, adiabatic, and cooling cases by pressures by fluid-structure interactions. A fully developed flow condition is supplied by the length of the pipe. The variation of density and viscosity is taken into account by the generated function. In this way, the variations of these parameters are considered for the fluid during the flow.

According to the results, the following evaluations were reached:

- When the thermal conditions of the pipe are assessed for the heating, adiabatic, and cooling cases, the deformations and stress are highly low according to the thermal process. The results near the inlet showed an abrupt rise due to developing flow.

Therefore developing flow significantly increases the investigated parameters in a turbulent flow.

- An increase in the pressure, for the same flow conditions at the constant surface temperature decreases heat transfer to the fluid so deformation and stress present a decrease along the pipe. This can be achieved by variable thermophysical properties of the fluid. Unless these results may vary and lead to unpredictable values.
- Developing flow increases the heat transfer from the pipe to the fluid and also increases the deformation and stress for the solid domain.
- Even though a rise in the temperature affects the solid domain to deformation, the variation of the thermophysical properties of the fluid compensates for this effect due to a decrease in the viscosity.

FSI analyses are highly important in investigating a solid domain interaction with a fluid to observe structural response because the variation of thermophysical properties of the fluid directly changes pressure distribution on the surface of the solid domain.

5. REFERENCES

1. Li, S., Karney, B.W., Liu, G., 2015. FSI Research in Pipeline Systems - A Review of the Literature. *J. Fluids Struct.*, 57, 277-297.
2. Mohammed, A.O., Al-Kayiem, H.H., A.B., O., Sabir, O., 2020. One-Way Coupled Fluid-Structure Interaction of Gas-Liquid Slug Flow in a Horizontal Pipe: Experiments and Simulations. *J. Fluids Struct.*, 97, 103083.
3. Tijsseling, A.S., 1996. Fluid-Structure Interaction in Liquid-Filled Pipe Systems: A Review. *J. Fluids Struct.*, 10, 109-146.
4. Darıcık, F., Canbolat, G., Koru, M., 2022. Investigation of a Fiber Reinforced Polymer Composite Tube by Two Way Coupling Fluid-Structure Interaction. *Coupled Syst. Mech.*, 11,315-333.
5. Etli, M., Canbolat, G., Karahan, O., Koru, M., 2021. Numerical Investigation of Patient-Specific Thoracic Aortic Aneurysms and

- Comparison with Normal Subject via Computational Fluid Dynamics (CFD). *Med. Biol. Eng. Comput.*, 59, 71-84.
6. Benra, F.-K., Dohmen, H.J., Pei, J., Schuster, S., Wan, B., 2011. A Comparison of One-Way and Two-Way Coupling Methods for Numerical Analysis of Fluid-Structure Interactions. *J. Appl. Math.* 2011, 1-16.
 7. Ahamed, M., Atique, S., Munshi, M., Koironen, T., 2017. A Concise Description of One Way and Two Way Coupling Methods for Fluid-Structure Interaction Problems. *Am. J. Eng. Res.*, 86-89 .
 8. Tijsseling, A.S., 2007. Water Hammer with Fluid-Structure Interaction in Thick-Walled Pipes. *Comput. Struct.*, 85, 844-851.
 9. Ferras, D., Manso, P.A., Schleiss, A.J., Covas, D.I.C., 2017. Fluid-Structure Interaction in Straight Pipelines with Different Anchoring Conditions. *J. Sound Vib.*, 394, 348-365.
 10. Sreejith, B., Jayaraj, K., Ganesan, N., Padmanabhan, C., Chellapandi, P., Selvaraj, P., 2004. Finite Element Analysis of Fluid-Structure Interaction in Pipeline Systems. *Nucl. Eng. Des.*, 227, 313-322.
 11. Zhu, H., Zhang, W., Feng, G., Qi, X., 2014. Fluid-Structure Interaction Computational Analysis of Flow Field, Shear Stress Distribution and Deformation of Three-Limb Pipe. *Eng. Fail. Anal.*, 42, 252-262.
 12. Elfaki, M., Nasif, M.S., Muhammad, M., 2021. Effect of Changing Crude Oil Grade on Slug Characteristics and Flow Induced Mechanical Stresses in Pipes. *Appl. Sci.*, 11.
 13. Zhu, H., Zhao, H., Pan, Q., Li, X., 2014. Coupling Analysis of Fluid-Structure Interaction and Flow Erosion of Gas-Solid Flow in Elbow Pipe. *Adv. Mech. Eng.*, 6, 815945.
 14. Guo, Q., Zhou, J.X., Guan, X.L., 2020. Fluid-Structure Interaction in Z-Shaped Pipe with Different Supports. *Acta Mech. Sin.*, 36, 513-523.
 15. Yunus A.J., Cimbala., M., 2006. *Fluid Mechanics Fundamentals and Applications*. Hill Higher Education, Boston, 1031.
 16. Canbolat, G., Yıldızeli, A., Köse, H.A., Çadircı, S., 2020. Düz Bir Plaka Üzerindeki Hidrodinamik ve Isıl Sınır Tabaka Akışının Sayısal Olarak İncelenmesi ve Geçiş Kontrolü. *Int. J. Adv. Eng. Pure Sci.*, 32, 390-397.
 17. Rzehak, R., Kriebitzsch, S., 2015. Multiphase CFD-Simulation of Bubbly Pipe Flow: A Code Comparison. *Int. J. Multiph. Flow.*, 68, 135-152.
 18. Elkarii, M., Boukharfane, R., Benjelloun, S., Bouallou, C., 2023. A CFD-Based Surrogate Model For Predicting Slurry Pipe Flow Pressure Drops. *Part. Sci. Technol.*, 41, 432-442.
 19. Canbolat, G., Etlı, M., Karahan, O., Koru, M., Korkmaz, E., 2023. Investigation of Vascular Flow in a Thoracic Aorta in Terms of Flow Models and Blood Rheology via Computational Fluid Dynamics (CFD), *J. Mech. Med. Biol.*, 2350094.
 20. Hughes, T.J.R., Liu, W.K., Zimmermann, T.K., 1981. Lagrangian-Eulerian Finite Element Formulation for Incompressible Viscous Flows. *Comput. Methods Appl. Mech. Eng.*, 29, 329-349.
 21. ANSYS, 2013. *Ansys Fluent Theory Guide*, ANSYS, Inc., 275 Technology Drive Canonsburg, 15317.
 22. Ezkurra, M., Ander Esnaola, J., Martinez Agirre, M., 2018. Analysis of One-Way and Two-Way FSI Approaches to Characterise the Flow Regime and the Mechanical Behaviour During Closing Manoeuvring Operation of a Butterfly Valve Structural Integrity of Offshore Renewable Energy Platforms View Project., 12, 409-415.
 23. Gorman, D.G., Reese, J.M., Zhang, Y.L., 2000. Vibration of a Flexible Pipe Conveying Viscous Pulsating Fluid Flow. *J. Sound Vib.*, 230, 379-392.
 24. Heinsbroek, A.G.T.J., 1997. Fluid-Structure Interaction in Non-Rigid Pipeline Systems. *Nucl. Eng. Des.*, 172, 123-135.
 25. Bureček, A., Hružík, L., Vašina, M., 2015. Simulation of Accumulator Influence on Hydraulic Shock in Long Pipe. *Manuf. Ind. Eng.*, 14, 1-4.
 26. Hružík, L., Bureček, A., Vašina, M., 2014. Non-Stationary Flow of Hydraulic Oil in Long Pipe. *EPJ Web Conf.*, 67, 1-5.